Jurnal Teknologi

Full paper

Numerical Analysis of Effect of Preheat and Swirl of Inlet Air on Temperature Profile in Canister Burner

Mohamad Shaiful Ashrul Ishak[a,b*], Mohammad Nazri Mohd. Jaafar[b], Wan Zaidi Wan Omar[b]

[a]*School of Manufacturing Engineering, Universiti Malaysia Perlis, P.O Box 77, Pejabat Pos Besar, 01000 Kangar, Perlis, Malaysia*
[b]*Department of Aeronautics, Automotive & Ocean Engineering, Faculty of Mechanical Engineering,Universiti Teknologi Malaysia, 81310 UTM Johor Bahru, Johor, Malaysia*

*Corresponding author: mshaiful@unimap.edu.my

Article history

Received : 15 August 2014
Received in revised form :
15 October 2014
Accepted :15 November 2014

Graphical abstract

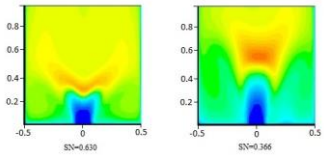

Abstract

The main purpose of this paper is to study the Computational Fluid Dynamics (CFD) prediction on temperature distribution inside the canister burner with inlet air pre-heating of 100K and 250K while varying the swirl angle of the radial swirler. Air swirler adds sufficient swirling to the inlet flow to generate central recirculation region (CRZ) which is necessary for flame stability and fuel air mixing enhancement. Therefore, designing an appropriate air swirler is a challenge to produce stable, efficient and low emission combustion with low pressure losses. A liquid fuel burner system with different radial air swirler with 280 mm inside diameter combustor of 1000 mm length has been investigated. Analysis were carried out using four different radial air swirlers having 30°, 40°, 50° and 60° vane angles. The flow behavior was investigated numerically using CFD solver Ansys Fluent. This study has provided characteristic insight into the distribution of temperature inside the combustion chamber. Results show that with the inlet air preheat before the combustion, the temperature distribution inside the canister would stabilize early into the chamber with higher swirl number (SN) compared without inlet air preheat. As for the inlet air preheat, the main effects are the resulting temperatures in the canister are higher, but there is a smaller hot-spot in the flame. This means that the temperature profile in the chamber is well distributed.

Keywords: Swirl combustion; can combustor; inlet air preheat; CFD simulation

1.0 INTRODUCTION

Swirling jets are used for the stabilisation and control of a flame and to achieve a high intensity of combustion. The common method of generating swirl is by using angle vanes in the passages of air. The characteristic of the swirling jet depends on the swirler vane angle [1, 2]. Various investigation on the effects of swirl on the flame stability for swirl flame in the unconfined space have shown increasing fuel/air mixing as the degree of swirl increased [3]. The size and strength of the central recirculation zone (CRZ) also increased with an increase in swirl intensity. At low flow rates or swirl numbers, long yellow and highly luminous flames are produced indicating poor fuel-air mixing [4]. However, when the swirl number is increased, the CRZ increases in size, initially in width until restricted by the diameter of the combustor and then begin to increase in length [4]. Measurements of the flame length and stabilization distance carried out in the series of butane-propane-air flames with swirl, have shown that both decrease markedly with increasing degree of swirl [5]. Tian on the other hand, numerically compared the effects of swirling and non-swirling system on combustion [6]. He demonstrated that the existence of swirl helps improve combustion efficiency, decreases all pollutants and increases flame temperature. He also observed that during the presence of a swirl, a shorter blue flame was observed indicating a short time for peak temperature resulting in good mixing while non-swirling system showed a longer yellow flame indicating a long time peak temperature, and there is still some fuel left un-vaporised. Increasing of swirl number improves the flame stability due to the presence of the recirculation zone [7]. Increasing the swirl number will increase the angle of the jet thereby increasing the total available surface area per unit volume of the jet. This allows further mixing with the surrounding fluid in the free jet and the central core of the flow [8]. It has also been shown that flames with low swirl have instability problems, because of the absence of the recirculation zone [9].

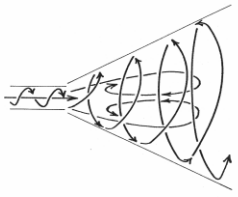

Figure 1 Jet flow of high degree of swirl (S > 0.6) resulting in significant lateral as well as longitudinal pressure gradients. Compared to its non-swirling counterpart, the jet is much wider, slower and there exist a central toroidal recirculation zone [9]

Figure 1 shows schematically a jet flow with high degree of swirl, which results in significant lateral as well as longitudinal pressure gradients. Compared to its non-swirling counterpart, the jet is much wider, slower and with a central toroidal recirculation zone. In combustion, the presence of this recirculation zone plays an important role in flame stabilization by providing a rearward hot flow of combustion products at the centre of the combustion chamber which is a reduced velocity region where flame speed and flow velocity can be matched. Swirls also act to shorten the flame length and this is advantageous for having more compact burner design [10].

The geometric swirl number (S_N) has been formulated by Al-Kabie [10] and given as;

$$S_N = \frac{\sin\theta}{1 + 1/\tan\theta}\left[\frac{A_a}{C_c A_{th}}\right] \quad (1)$$

Where

A_a is the swirler exit area
A_{th} is the swirler minimum throat area
C_C is the swirler contraction coefficient

Value for C_C, the swirler contraction coefficient, C_D, the swirler discharge coefficient and hence the swirl number was obtained using the following Equation (2) and Equation (3). The discharge coefficient in term of swirler pressure drop and air mass flow rates can be obtained as;

$$C_D = \frac{\dot{m}}{A_{th}\sqrt{2\rho\Delta P}} \quad (2)$$

Where

$\dot{m}$ is the volumetric air flow rates
ΔP is the pressure drop

An expression for contraction coefficient in term discharge coefficient, throat area and swirler exit area can be obtained as follow;

$$C_C = \frac{C_D}{1 + \left(\frac{C_D A_{th}}{A_a}\right)} \quad (3)$$

The swirl number should, if possible, be determined from measured values of velocity and static pressure profiles. However, this is frequently not possible due to the lack of detailed experimental results. Therefore, it has been shown that the swirl number may be satisfactorily calculated from geometry of most swirl generator [11].

The main focus of this research is to investigate the effect of air pre-heating at inlet to the temperature distribution while varying the swirl angle inside the combustor. In this paper, flow pattern characteristics of temperature profile which are the main characteristics of the swirling flows, are studied to understand the physical processes by modelling the flow using Ansys CFD software. An assumption has been made in this research as that is the combustion mass flow rate is equal.

■2.0 MODELING, MESHING AND BOUNDARY CONDITION

The basic geometry of the gas turbine can combustor is shown in Figure 2 and Figure 3. The size of the combustor is 1000 mm in the Z direction, 280 mm in the X and Y direction. The primary inlet air is guided by radial curve vanes swirler to give the air a swirling velocity component. Standard Ansys database of liquid diesel ($C_{10}H_{22}$) is injected at the center of swirler. The transverse analysis is focused downstream of the swirler in the expansion chamber at various cross section stations (z/D = 0.2 to 1.0) as shown in Figure 3. Four different vane angles of 30º, 40º, 50º and 60º with the swirl number, SN of 0.366, 0.630, 0.978 and 1.427 respectively, were analyzed numerically at different boundary conditions to show the effects of the swirler configurations on the turbulence production, recirculation zone and also pressure loss. The intake condition for the combustion simulation is at stoichiometry. The inlet air were supply at 300K for combustion without pre-heating and increased 100K and 250K for two others cases. The technical data of the four swirlers used in this study are listed in Table 1.

The physical domains of the radial swirlers were decomposed to several volumes to facilitate meshing with cooper hexahedral structured grid. The geometry meshing was done to have a variable density distribution by mean of small mesh size which was incorporated in high gradient zone and bigger size in low gradient zone. The combustor model meshing for the present work is shown in Figure 4. The resulting base mesh is contains approximately 0.6 million cells, which were then applied in this simulation work and presented in this paper.

In the present simulation, k-epsilon turbulence model was used. Turbulence is represented by the realizable k-epsilon model, which provides an optimal choice and economy for internal turbulent flows [12].

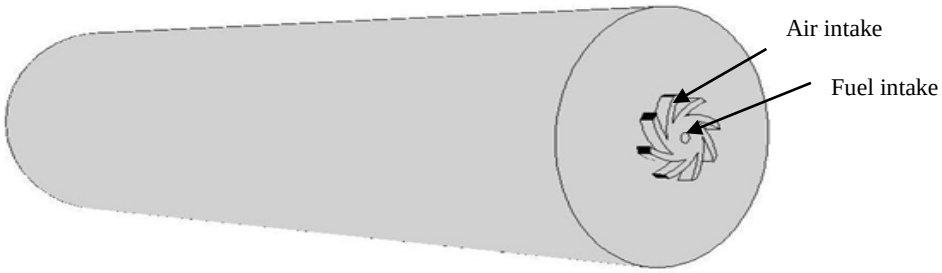

Figure 2 Combustor model

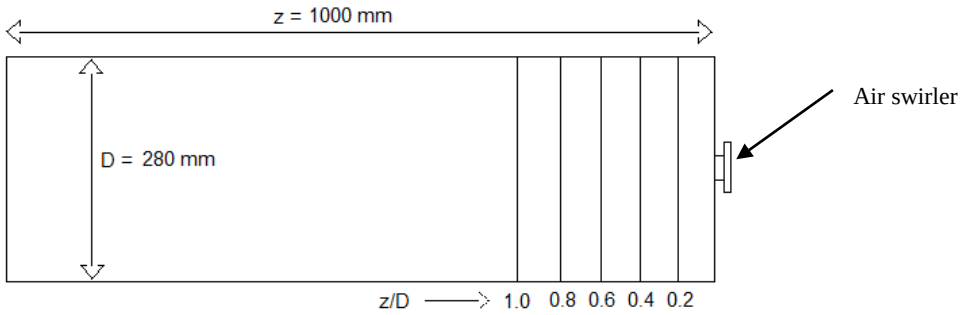

Figure 3 Details of position of transvers measuring stations indicated by cross section lines (z/D = 0.2 to 1.0) from the swirler throat

Table 1 Technical data of the swirlers

Swirler angle	30°	40°	50°	60°
Swirl No. (SN) (Based on numerical results)	0.366	0.630	0.978	1.427
Passage width, *h* (mm)	13.6	12.3	11.2	9.6
Hub diameter, *d* (mm)	50			
Outer diameter, *D* (mm)	98			

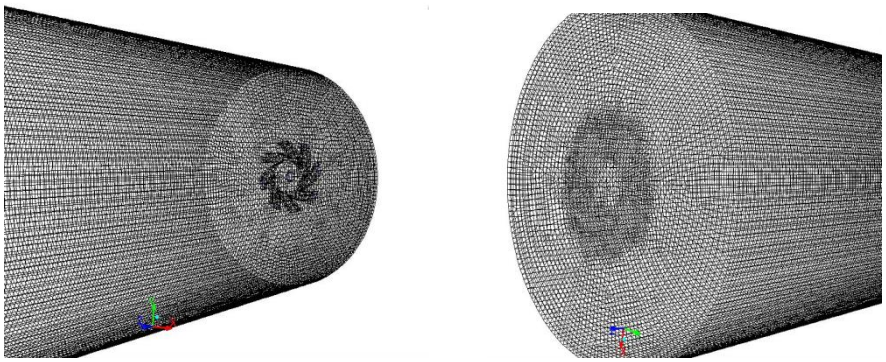

Figure 4 Combustor model meshing

The boundary conditions for this simulation are the inlet, standard wall function and the outlet as the boundaries. At the inlet of the computational region, the inlet boundary condition is defined as mass flow inlet for air supply and fuel nozzle while the exit boundary is defined as outflow. Some assumptions for boundary conditions that were not directly measured had to be made as follows:

i. Velocity components and turbulence quantities at the inlet were constant throughout the cross section;
ii. Turbulence at inlet is calculated from the following equations [13]:

$$k_{inlet} = 0.002(u^2)_{inlet} \quad (6)$$

$$\varepsilon = \frac{k_{inlet}^{1.5}}{0.3D} \quad (7)$$

where, u is the axial inlet flow velocity and *D* is the hydraulic diameter.

A collection of physical models was used to simulate the turbulent liquid fuel reacting flows. These models were selected due to their robustness and accuracy for industrial applications.

Turbulence Model: The current study uses the realizable *k–ε* turbulence model. This model is in the class of two-equation models in which the solution of two separate transport equations allows the turbulent velocity and length scales to be independently determined. The realizable *k–ε* turbulence model is robust, economic and reasonably accurate over a wide range of turbulent flow. The realizable *k–ε* turbulence model solves transport equations for kinetic energy (*k*) and its dissipation rate (*ε*). It assumes that the flow is fully turbulent, and the effects of molecular viscosity are negligible. The realizable *k–ε* turbulence model is therefore valid for fully turbulent flows, consistent with the flow characteristics in a typical combustion chamber.

Combustion Models: Combustion models are characterized by the type of mixing (e.g. non-premixed, premixed or partially premixed) and the reaction chemistry (e.g. finite-rate chemistry or fast chemistry). Liquid fuel combustion primarily takes place in a diffusion-limited mode (non-premixed) where fuel and oxidant are brought into contact via mixing and then react. In

these types of flames, it can generally be assumed that the turbulent mixing rate is much slower than the chemical kinetics rates (fast chemistry), and hence, will be the rate-limiting step. The current study used the eddy-dissipation combustion model, which assumed that the reaction rate is controlled by the turbulent mixing rate. Hence, the turbulent mixing rate in conjunction with a global reaction mechanism is used to predict local temperatures and species profiles. This model solves the conservation equations describing convection, diffusion, and reaction sources for each component species.

3.0 RESULTS AND DISCUSSION

Transversal profiles of gas-phase temperatures were obtained from the simulations at 56 mm (z/D=0.2), 112 mm (z/D=0.4), 168 mm (z/D=0.6) and 224 mm (z/D=0.8) from the swirler throat exit position as seen in Figures 5 to 10. In total, four radial swirler produced flames were investigated without air preheat and with air preheat of 100K and 250K. Four swirlers were used producing swirl numbers of 0.366, 0.630, 0.978 and 1.427.

The effect of the swirler on temperature distribution inside the combustor could be analyzed from the different profiles as the flow progresses from the exit of the swirler nozzle along the axis of the combustor. Immediately after the swirler exit (z/D=0.2), the temperature distribution for high swirler nozzle is well distributed across the combustor cross section but for low swirl nozzle the high temperature is concentrated at area away from core. The central part of the cross-section suffers from low temperatures indicating no combustion occurring at that point. As the flow progresses along the combustor to z/D=0.8, the core temperature for the all the swirlers became equally distributed across the section except swirler with SN=0.366. For this swirler the flame is still active at cross section z/D=0.8, causing the uneven temperature distribution at this point. For high swirl, the flame is wide and short, thus the temperature becomes equally distributed at earlier sections (z/D=0.4 for SN=1.427, z/D=0.6 for SN=0.630 and 0.978), this explanation tallies with Figure 5.

For the preheat cases of 100K and 250K the results show that with preheat and swirl, the combustion produced maximum temperature at point nearer to the burner throat. Figures 6 and 7 show that for SN=0.630, the maximum temperature was attained after z/D=0.2 for flows without preheat but for preheated flows, the maximum temperature was reached before this point. These agree with Khalil and Gupta who studied swirl preheated combustion experimentally [14]. For the preheat cases for SN=0.630, 0.978 and 1.427, it can be clearly seen that the temperature profile for high swirl stabilizes at earlier axial distance. It also suggests that the pre-heating of inlet air improve the swirl performance in the combustion chamber. This can be seen in the figures where, without preheat, the temperature profile stabilizes at axial distance past z/D=0.6 meanwhile when pre-heated by 100K the temperature profile stabilizes at z/D=0.4.

The effect of swirl can also be seen in the plots of temperature profiles which stabilizes earlier as the swirl number (SN) increases. In the non-preheat case, the temperature profile for SN=0.978 and SN=1.427 stabilized at z/D=0.4 whereas for SN=0.630, it stabilized at z/D=0.6. For the lower swirl with SN=0.366, the temperature did not stabilizes even z/D=0.8.

The Figure 8 to 10 shows the temperature contour across the sections along axial axis. The effects of the swirler without preheated on the flame buoyancy are shown in Figure 8. High swirl flows will produce short but wide flame, thus reducing the time and distance for burning. It also reduces the peak temperatures due to the flame, such that the whole combustion temperature does not reach the point where NOx starts to form. For combustions with low swirl, the buoyancy of the flame is high, meaning the flame is concentrated in the core flow, but occurs at further axial distance from the exit of the swirler throat. This happens because the lower swirl flow reduces the mixing efficiency if the fuel with the air. In addition, low swirl also results in faster axial core flow. This pushes the combustion zone away from the swirler throat, increasing the buoyancy of the flame. The flame is also longer, thus creating a region of high intense heat at the core of the chamber away from (up to z/D=0.8) from the swirler throat. For the preheated cases of 100K and 250K, the trend is the same for the case when inlet air was not pre-heated.

The effects of pre-heat are very prominent with low swirl flow. In low swirl flow, there exists a large concentrated hot point where the temperature is 2100K. This hot-spot is reduced in size for the same flow condition with increasing inlet air pre-heat temperatures. At pre-heat temperature of 100K the maximum temperature are 2100K but the size of heat concentration area is well reduced as seen in Figures 9 and 10.

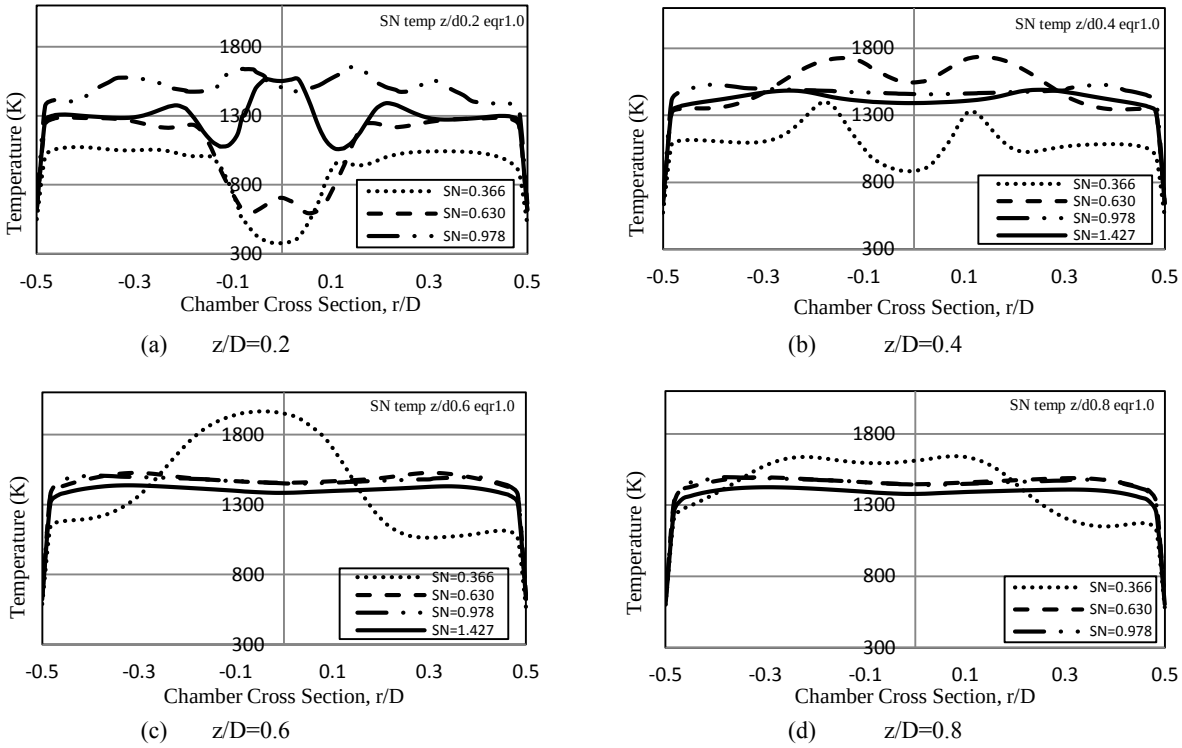

Figure 5 Transversal mean gas temperature profile without pre-heat at different axial stations

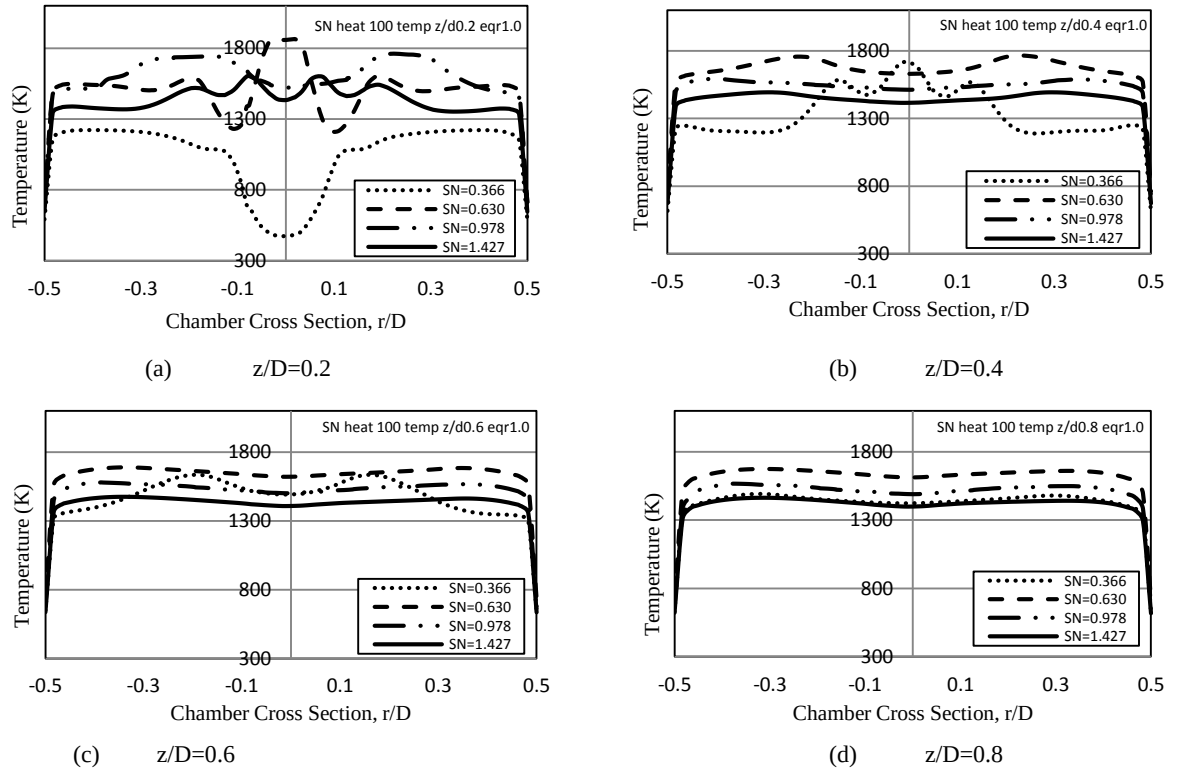

Figure 6 Transversal mean gas temperature profiles with 100K inlet pre-heat at different axial stations

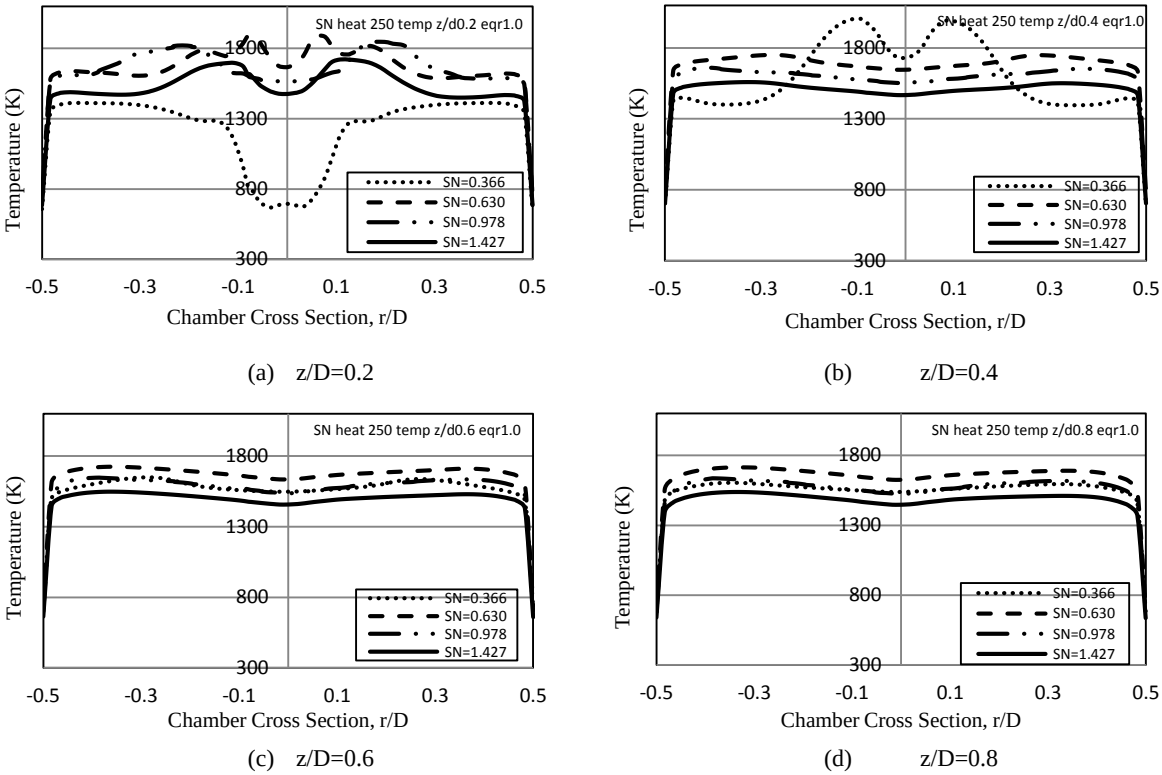

Figure 7 Transversal mean gas temperature profiles with 250K inlet pre-heat at different axial stations

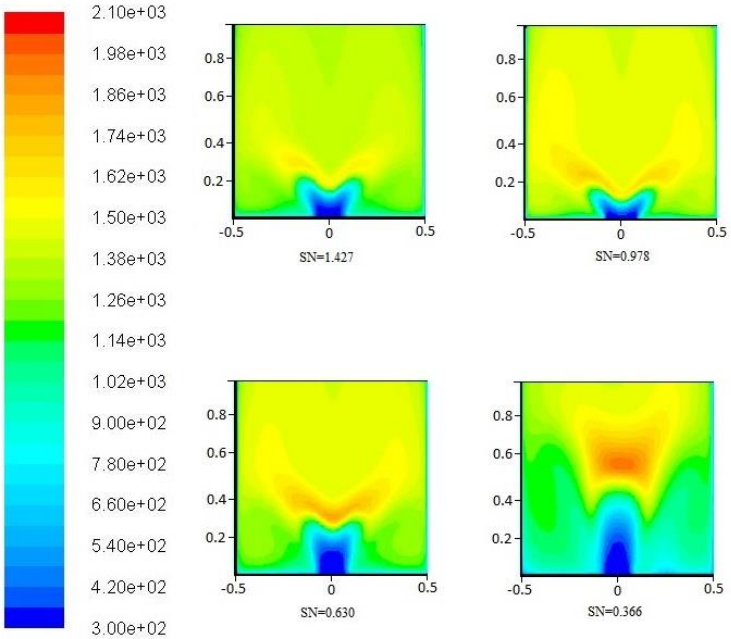

Figure 8 Effect of swirl number on the temperature contour in combustor the combustor without inlet air pre-heat (Scale in Kelvin)

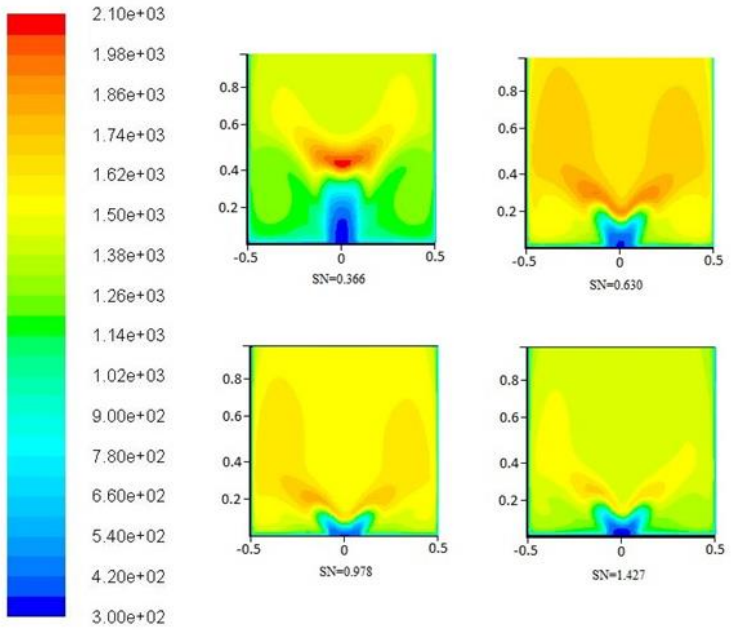

Figure 9 Effect of swirl number on the temperature contour in combustor the combustor with 100K inlet air pre-heat (Scale in Kelvin)

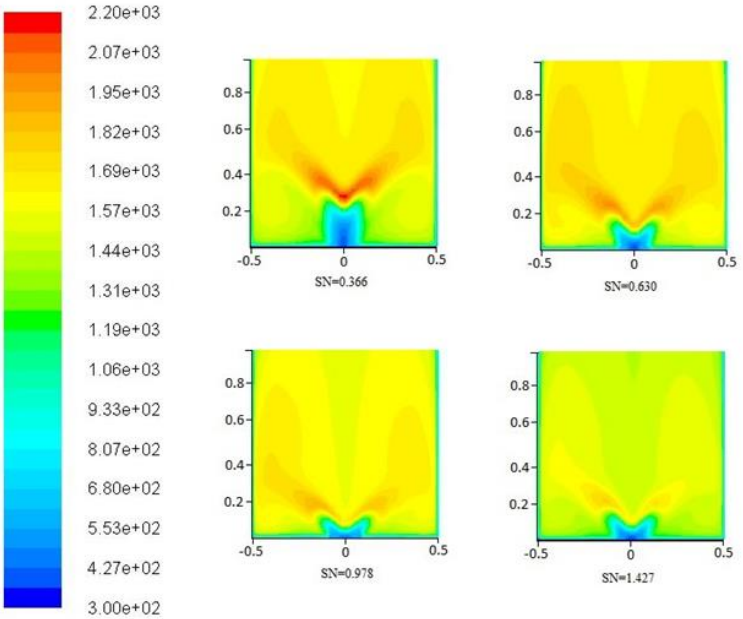

Figure 10 Effect of swirl number on the temperature contour in combustor the combustor with 250K inlet air pre-heat (Scale in Kelvin)

4.0 CONCLUSION

The CFD simulation of combustion in canister burner was conducted with varying intake air swirl and preheats temperature. The main effects of swirl are that the temperature distribution inside the canister would stabilize early into the chamber with higher swirl number (SN) compared without inlet air preheat. As for the inlet air preheat, the main effects are the resulting temperatures in the canister are higher, but there is a smaller hot-spot in the flame. This means that the temperature profile in the chamber is well distributed. The preheat also stabilize the flow at an earlier axial distance from the intake point.

Acknowledgement

The authors would like to thank the Ministry of Higher Education of Malaysia & Research Management Center (project number: 01G60) for awarding a research grant to undertake this project. The authors would also like to thank the Faculty of Mechanical Engineering, Universiti Teknologi Malaysia for providing the research facilities and space to undertake this work.

References

[1] Mathur, D. L. 1974. A New Design of Vanes for Swirl Generation. *IE (I) Journal Me*. 55: 93–96.
[2] Jaafar, M. N. M., Ishak, M. S. A., Saharin, S. 2010. Removal of NOx

and CO from a Burner System. *Environmental Science and Technology*. 44 (8): 3111–3115.

[3] Fricker, N. and Leuckel, W. 1976. The Characteristic of Swirl Stabilized Natural Gas Flame Part 3: The Effect of Swirl and Burner Mouth Geometry on Flame Stability. *J. Inst. Furl*. 49: 152–158.

[4] Mestre, A and Benoit, A. 1973. Combustion in Swirling Flow. *14th Symposium (International) on Combustion, The Combustion Institute*. Pittersburg. 719.

[5] Chervinskey, A. and Manheimertiment, Y. 1968. Effect of Swirl on Flame Stabilization. *Israel Journal of Technology*. 6(2): 25–31.

[6] Tian, Z. F., Witt, P. J., Schwarz, M. P., & Yang, W. 2010. Numerical Modelling of Victorian Brown Coal Combustion in a Tangentially Fired Furnace. *Energy & Fuels*. 24(9): 4971–4979.

[7] Khalil, K. H., El-Mehallawy, F. M. and Moneib, H. A. 1977. Effect of Combustion Air Swirl on the Flow Pattern in a Cylindrical Oil Fired Furnace, *16th Symposium (International) on Combustion, The Combustion Institute, Pittersburg*. 135–143.

[8] Apack, G. 1974. Interaction of Gaseous Multiple Swirling Flames, Phd thesis, Department of Chemical Engineering and Fuel Technology, University of Sheffield.

[9] Gupta, A. K., Lilley, D. G. and Syred, N. 1984. *Swirl Flows*. Abacus Press, Tunbridge Wells, England.

[10] Al-Kabie, H. S. 1989. *Radial Swirlers for Low Emissions Gas Turbine Combustion*. University of Leeds, Dept. of Fuel & Energy: PhD.

[11] Beer, J. M., Chigier, N. A. 1972. *Combustion Aerodynamics*. Applied Science Publisher, London.

[12] Kim, Y. M., Chung, T. J. 1989. Finite- Element Analysis of Turbulent Diffusion Flames. *AIAA J*. 27(3): 330–339.

[13] Versteeg, H. K., Malalasakera, W. 1995. *An Introduction to Computational Fluid Dynamics, the Finite Volume Method*. Longman Group Ltd.

[14] Khalil, A. E., & Gupta, A. K. 2011. Distributed Swirl Combustion for Gas Turbine Application. *Applied Energy*. 88(12): 4898–4907.